

Research note
23rd International Meshing Roundtable (IMR23)

Segmentation of the Visible Human Project® (VHP) Female Cryosection Images within MATLAB® Environment

J. Yanamadala^{a,*}, V. K. Rathi^a, S. Maliye^a, H. A. Win^a, A. L. Tran^a, M. K. Kozlov^b,
G. M. Noetscher^{a,c}, A. Nazarian^d, and S. N. Makarov^{a,c}

^aECE Dept., Worcester Polytechnic Institute, Worcester, 01609 MA, USA

^bMax Plank Institute for Human Cognitive and Brain Sciences, Leipzig, Germany

^cNEVA Electromagnetic LLC, Yarmouth Port, 02675 MA, USA

^dBeth Israel Deaconess Medical Center, HMS, 330 Brookline Ave, Boston, MA 02215

Abstract

The subject of this study is triangular surface image segmentation within MATLAB environment. The goal has been an attempt to create a whole-body human phantom from the Visible Human Project® (VHP) dataset. The original result of this study is the mesh intersection algorithm for manifold tissue meshes based on a constrained 2D Delaunay triangulation in MATLAB.

Keywords: Image segmentation; MATLAB®; Visible Human Project® (VHP); triangular surface meshes; mesh intersection

1. Image source and prior segmentation efforts with ITK-SNAP and MeshLab

The model utilized in this study was constructed using anatomical cryosection images taken in the axial plane provided as part of the Visible Human Project® (VHP) established in 1989 by the U.S. National Library of Medicine (NLM) [1]. Male and female data sets became available in November of 1994 and 1995, respectively. Each consisted of MRI, CT and cryosection images taken predominantly in the axial plane of the bodies at various resolutions.

* Corresponding author. Tel.: +1-774-578-5948;
E-mail address: jyanamadala@wpi.edu

Anatomical cryosection image data from the female patient, consisting of 2048 by 1216 pixels with each pixel measuring 0.33mm per side, was used in the construction of the model for the present study, producing the VHP-Female nomenclature.

One of the major tools developed in conjunction with the VHP dataset and utilized to create the original VHP triangular surface meshes [2] was the open source program Insight Toolkit-SNAP (ITK-SNAP) [3], which enables the analysis of three dimensional image stacks and simultaneous segmentation of images in the axial, coronal, and sagittal body planes via manual and automatic methods. The user may manually trace organs, tissues and other structures. The end result is a stereolithography (STL) file describing the surface of the segmented region as a dense triangular mesh.

Much of the mesh conditioning process has been accomplished via the open source program MeshLab [4]. Example operations include selective reduction of the number of nodes via quadric edge collapse decimation [5], surface-preserving (HP) Laplacian smoothing [6], Poisson surface reconstruction [7], etc.

Following the segmentation and conditioning processes, all individual components of the VHP-Female model were registered to ensure proper position, size and shape. Registration was accomplished by overlaying the digitized structures on top of the original cryosection images and any required adjustments were made on a node by node or element by element basis. The resulting surface reconstruction error (deviation of the triangulated surface from the physical surface) does not exceed 2 mm on the human head and 5 mm otherwise. The initial VHP-Female model constructed with ITK-SNAP and MeshLab contained 33 individual tissues describing the human head and torso (with superior resolution on the human head, including the continuous CSF shell) and was recently used for research purposes related to electromagnetic modelling [8]-[9]. In 2014, this partial model was evaluated and accepted by the IEEE International Committee on Electromagnetic Safety for calculation of Specific Absorption Rates (SARs) [10]-[11].

2. Outline of segmentation/surface reconstruction workflow in MATLAB

The latest basic MATLAB platform (without toolboxes) has a number of built-in and open-source features that makes it an accessible alternative for medical image segmentation and surface reconstruction. These features relate to both computational geometry and image processing. In particular, they include (compatibility with R2015a):

- Pixel-based image processing tools: resampling, registration, mouse I/O (functions `imread`, `imagesc`, `ginput`);
- 3D Delaunay triangulation or tetrahedralization, constrained and unconstrained 2D Delaunay triangulations (`delaunay`, `triangulation`);
- 3D surface mesh generation via a sculpting based volumetric method [12] or a region-growing surface method – the ball-pivoting method [13] (an excellent function `MyRobustCrust` by Dr. L. Giaccari);
- 3D surface-preserving mesh decimation (via the function `reducepatch`)
- Interactive mesh processing tools such as selection of vertices or triangles of a 3D surface mesh and visualization of multiple meshes in many different formats (function `select3d` by Dr. J. Conti).

The goal of the present study has been to establish a segmentation and surface reconstruction workflow to enhance and augment the VHP-Female model entirely in MATLAB. The corresponding workflow, separated into short MATLAB scripts, is outlined in Fig. 1 and includes:

- Data acquisition (scan data) of the body in the xy-plane using one of a set of images;

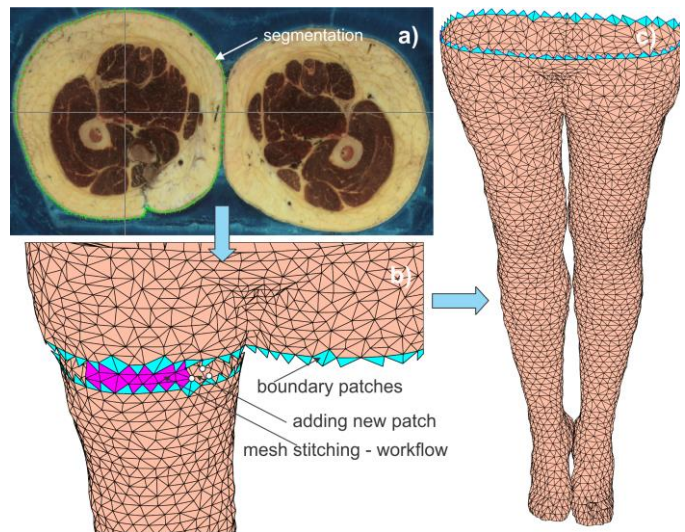


Fig.1 Illustration of the segmentation/mesh generation workflow: a) – segmentation; b) – stitching of two individual surface meshes; c) – semi-complete surface mesh.

- Manual mouse selection of nodes indicating a boundary of interest (segmentation) using 2D mouse input *ginput*. Left click adds a nodal point; right click deletes the previous node, hitting return acquires the next image;
- 3D surface mesh generation via the ball-pivoting method as implemented in the function *MyRobustCrust*;
- Automatic selection and visualization of edges with only one adjacent triangle (hole boundaries) and with more than two adjacent triangles (non-manifold edges);
- Sequential selection of individual triangles/nodes/edges using function *select3d*. Manual removal/addition of selected triangles, mesh stitching, mesh healing;
- Mesh smoothing and mesh coarsening using *reducepatch*.

3. Mesh intersection algorithm for 2 manifold triangular meshes via constrained 2D Delaunay triangulation

An important problem in human body segmentation is related to intersections of meshes describing different tissues after surface reconstruction. We were unable to find public-domain MATLAB codes that implement one of the existing intersection algorithms [14]-[19]. An original algorithm has therefore been developed and tested. In contrast to the classic paper [14] and other relevant sources [15], [16], [19], we do not explicitly construct the chains and loops of intersection line segments. Instead, all individual intersection line segments are collected randomly and then a constrained 2D Delaunay triangulation is applied to each triangle with the intersection line segments separately. Note that the constrained 2D Delaunay triangulation was also used in [19], but augmented with the construction of intersection chains. The algorithm steps are as follows (the goal is to subtract a manifold Y from a manifold X):

- For every edge of mesh X, find the triangle(s) of mesh Y intersected by this edge and the corresponding intersection points via Möller & Trumbore algorithm [20] vectorized in MATLAB. Store the results in two distinct cell arrays.
- Swap meshes X and Y and perform the same operation.
- For every triangle of mesh X falling into the intersection list, collect all extra line segments (node pairs) to be added. Three scenarios are possible. The first is when *two* edges of a triangle in Y intersect the triangle in X. A line segment $Q_{11}Q_{12}$ in Fig. 2 has to be added. The second scenario is when only *one* edge of a triangle in Y intersects the triangle in X. Then, an edge of the triangle in X must also intersect this triangle in Y. A line segment $Q_{21}Q_{22}$ in Fig. 2 has to be added. The last scenario is when two edges of the triangle in X intersect a certain triangle in Y. A line segment $Q_{31}Q_{32}$ in Fig. 2 has to be added. Finally, store all results in a cell array.
- Swap meshes X and Y and perform the same operation.
- For every triangle of mesh X falling into the intersection list, remove duplicated nodes/remunerate the constrained line segments using function *unique* with three arguments and perform constrained 2D Delaunay triangulation in MATLAB in the triangle plane. The local orthogonal coordinate system includes one (the longest) triangle edge as an x-axis. Remove sub-triangles of vanishingly small areas, which are routinely produced when multiple (intersection) points are located on the same edge of the triangle in X.
- Collect all sub-triangles in X and create a new refined mesh XR, which respects all the intersection segments and does not have duplicated points.
- Swap meshes X and Y and perform the same two previous operations.
- Using the original manifold X, determine all triangles YX of the refined mesh YR in X. Use the Möller & Trumbore algorithm [20] for triangle centers.
- Using the original manifold Y, determine all triangles XY of the refined mesh XR not in Y. Use the Möller & Trumbore algorithm [20] for triangle centers.
- Combine meshes XY and YX, eliminate duplicated points, and obtain the conformal mesh X-Y.

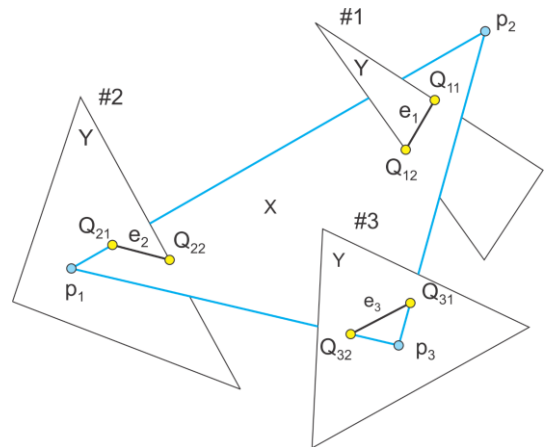


Fig.2 Three types of triangle intersections between a master mesh X and various triangles of a slave mesh Y. Cases #1 and #3 are equivalent if we treat the master and slave meshes as one set of triangles.

- Check if the mesh X–Y is a 2 manifold mesh without holes.

The above algorithm in its present form is straightforwardly programmed in MATLAB and shows a high reliability. It produces an exact representation of any curved intersecting surfaces. At the same time, it is yet to be optimized for speed and for handling of some degenerate cases. The default MATLAB precision is used. Two expected and undesirable results of this algorithm include potential reduction in the triangle quality due to the possible generation of low-quality (highly skewed) triangles and in an increase in the overall mesh size, which may be substantial for small-size meshes.

Vertices of intersecting meshes X and Y located in close proximity are the major source of both problems. Therefore, one way to address both issues identified above is to make those vertices coincident at the onset of the algorithm, immediately after identifying the intersections.

Yet another way is to apply mesh decimation on flat surfaces followed by local Laplacian smoothing, which slightly shrinks the selected surfaces in the direction of the inner surface normal vector. This operation leaves a gap between the intersected meshes. Since the distinct organ meshes are in fact separated by thin tissues, such a gap may be anatomically correct.

4. Results

Using the algorithm described above, we have treated multiple intersection cases such as inflated lungs/ribcage, white matter/CSF ventricles, etc. As a validation step, all meshes have passed the ANSYS High Frequency Structural Simulator (HFSS) mesh check at the strictest setting and Fig. 3 shows the present version of the VHP-Female model with over 80 parts. We are currently attempting to convert our triangular meshes to non-uniform rational basis spline (NURBS) representation. The corresponding efforts will be reported in future works.

Acknowledgements

We would like to acknowledge the contributions of Mr. A. T. Htet, Mr. J. M. Elloian, and Ms. V. Karna.

References

- [1] U.S. National Library of Medicine, The Visible Human Project®, Online: http://www.nlm.nih.gov/research/visible/visible_human.html.
- [2] G.M. Noetscher, The VHP-F Computational Phantom and its Applications for Electromagnetic Simulations, PhD Thesis, Worcester Polytechnic Institute, Apr. 2014, 307 p.
- [3] P. A. Yushkevich, J. Piven, H. C. Hazlett, R. G. Smith, S. Ho, J. C. Gee, G. Gerig, User-guided 3D Active Contour Segmentation of Anatomical Structures: Significantly Improved Efficiency and Reliability, *NeuroImage*. vol. 31 (2006) 1116-28.
- [4] Online: <http://meshlab.sourceforge.net>.
- [5] M. Garland, Quadric-Based Polygonal Surface Simplification, PhD Thesis, Pittsburgh, PA, 1999.
- [6] J. Vollmer, R. Mencl, H. Mueller, Improved Laplacian smoothing of noisy surface meshes, *Eurographics*. vol. 18 (1999) 1-8.
- [7] M. Kazhdan, M. Bolitho, H. Hoppe, Poisson Surface Reconstruction, *Eurographics Symposium on Geometry Processing*, 2006.
- [8] J.M. Elloian, G.M. Noetscher, S.N. Makarov, A. Pascual-Leone, Continuous wave simulations on the propagation of electromagnetic fields through the human head, *IEEE Trans. Biomedical Engineering*, vol. 61, no. 6 (June 2014) 1676-1683.
- [9] G. M. Noetscher, J. Yanamadala, S. N. Makarov, A. Pascual-Leone, Comparison of cephalic and extracephalic montages for Transcranial Direct Current Stimulation - A numerical study, *IEEE Trans. Biomedical Engineering*, vol. 61, no. 9 (Sep. 2014) 2488-2498.
- [10] IEEE International Committee on Electromagnetic Safety: Technical Committee 34: Wireless Handset SAR Certification Brochure. Online: <http://grouper.ieee.org/groups/scc34/sc2/>.
- [11] IEEE International Committee on Electromagnetic Safety: Technical Committee 34: List of approved human phantoms, Online: <http://grouper.ieee.org/groups/scc34/sc2/wg2/available%20human%20models.doc>.
- [12] C. Bajaj, F. Bernardini, G. Xu, Automatic reconstruction of surfaces and scalar fields from 3D scans, *Computer Graphics Proceedings*, 1995, Annual Conference Series. Proceedings of SIGGRAPH 95, pp. 109–118.
- [13] F. Bernardini, J. Mittleman, H. Rushmeier, C. Silva, G. Taubin, The ball pivoting algorithm for surface reconstruction, *IEEE Trans. Visualization and Computer Graphics*, vol. 5, no 4 (Oct-Dec. 1999).
- [14] S. H. Lo, Automatic mesh generation over intersecting surfaces, *Int. J. Numerical Methods Eng.*, vol. 38 (1995) 943–954.
- [15] S. H. Lo and W. X. Wang, A fast robust algorithm for the intersection of triangulated surfaces, *Engineering with Computers*, vol. 20 (2004) 11–21.
- [16] A. H. Elsheikh, M. Elsheikh, A reliable triangular mesh intersection algorithm and its application in geological modelling, *Engineering with Computers*, vol. 30 (2014) 143–157.
- [17] L. C. Coelho, M. Gattass, L. H. De Figueiredo, Intersecting and Trimming Parametric Meshes on Finite-Element Shells, *Int. J. for Numerical Methods in Engineering*, vol. 0(0) (1999) 1–100.

- [18] W. M. Lira, L. C. G. Coelho, L. F. Martha, Multiple Intersections of Finite-Element Surface Meshes, 11th International Meshing Roundtable, Ithaca, New York, USA, Sep. 15-18, 2002.
- [19] C.H. Lindenbeck, H.D. Ebert, H. Ulmer, L. Pallozzi Lavorante, R. Pflug, TRICUT: a program to clip triangle meshes using the rapid and triangle libraries and the visualization toolkit, Computers & Geosciences, vol. 28 (2002) 841–850.
- [20] T. Möller and B. Trumbore, Fast, Minimum Storage Ray/Triangle Intersection, J. of Graphics Tools, vol. 2 (1997) 21–28.

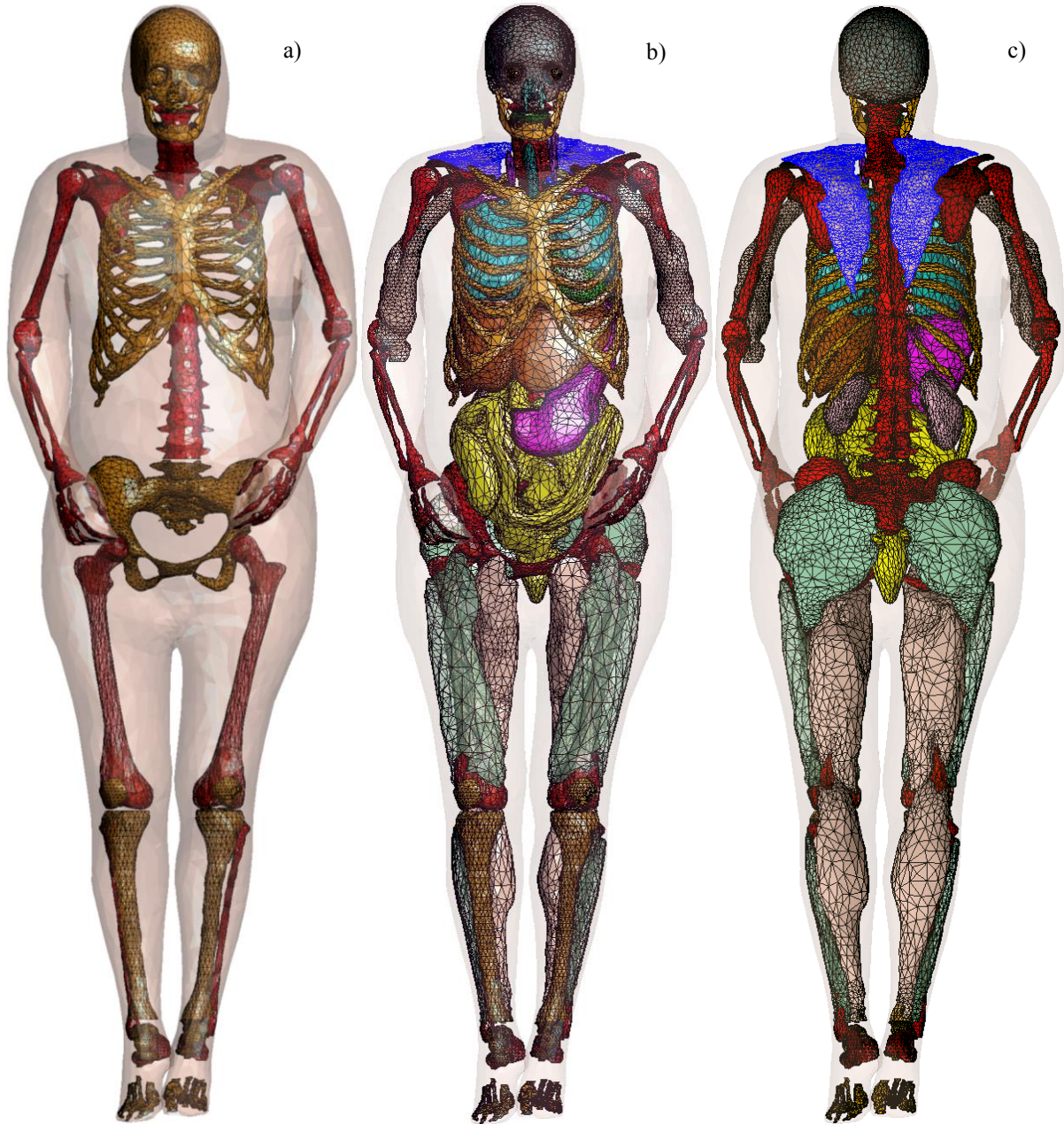


Fig.3 Partial VHP-Female model to date: a) – skeleton bones, b) – anterior view of organs and muscles, c) – posterior view of organs and muscles.